Tabelle 3. *Gitterkonstantenbeziehungen von Dihydrat, Übergangsphase und β-$NaVO_3$ auf der Basis der Dihydratzelle (vgl. Fig. 3)*

Umrechnungsmatrix für das β-$NaVO_3$: $(00\bar{2}/010/\frac{1}{2}0\frac{1}{2})$.

	a(Å)	b(Å)	c(Å)	β(°)
Dihydrat	16,756	3,6391	8,023	111,18
Übergangsphase	13,96	3,64	7,88	111,1
β-$NaVO_3$	10,728	3,6496	7,565	110,76

Wasserstoffbrücken zwischen den Schichten allmählich durch die Ionenbindungen O–Na–O ersetzt, was die Verschmelzung der Schichten bewirkt. Hierbei gehen die VO_3-Doppelketten wenig verändert in die β-$NaVO_3$-Struktur über, während die Oktaedersäulen total zerstört werden. Die Koordination um das Na-Ion erleidet in der β-$NaVO_3$-Struktur eine starke Verzerrung. Die Spur des ehemaligen Schichtenbaus ist dort noch an den Reihen der VO_3-Ketten parallel $(10\bar{1})_\beta$ erkennbar. Der Schichtabstand wird, parallel $\mathbf{a}_H$ gemessen, auf $c_\beta = 5{,}364$ Å reduziert.

Die Zwischenstufe stellt wahrscheinlich denjenigen Zustand dar, in dem sich die Entwässerung bei jedem zweiten Schichtpaar vollzogen hat. Denn die Länge der a_I-Achse 13,96 Å stimmt relativ genau mit der Summe von $a_H/2 = 8{,}378$ Å und $c_\beta = 5{,}364$ Å (den Schichtabständen vor bzw. nach der Entwässerung) überein. Die gegenseitigen Beziehungen zwischen den drei Gittern sind in Tabelle 3 zusammengestellt. In Richtung $\mathbf{c}_H$ bzw. $\mathbf{c}_I$ verringert sich die Gitterperiode wie folgt:

$$[001]_H \xrightarrow[-2\%]{} [001]_I \xrightarrow[-4\%]{} [101]_\beta.$$

Die Zwischenstufe besitzt vermutlich die Zusammensetzung $NaVO_3.H_2O$. Eine mögliche strukturelle Ähnlichkeit mit $KVO_3.H_2O$ (Christ, Clark & Evans, 1954; Evans, 1960), welches ebenfalls VO_3-Doppelketten parallel [001] und die Raumgruppe *Pnam* besitzt, ist unwahrscheinlich, da sich die Gitterkonstanten $a = 8{,}151$, $b = 13{,}586$ und $c = 3{,}697$ Å nicht mit denen der Na–Verbindung korrelieren lassen.

Während die Strukturen des Dihydrats und des β-$NaVO_3$ durch VO_3-Doppelketten durch fünffach koordinierte V-Atome gekennzeichnet sind, weist die Struktur der α-Form einfache VO_3-Ketten von über gemeinsame Ecken miteinander verknüpften VO_4-Tetraedern auf und ist somit mit den beiden erstgenannten Strukturen kaum verwandt. Die Umwandlung $\beta \rightarrow \alpha$ bzw. $\alpha \rightarrow \beta$ benötigt eine Umgestaltung der VO_3-Ketten, die in tieferem Temperaturbereich wahrscheinlich nur sehr langsam geschehen wird. Es ist daher verständlich, dass die von Lukács & Strusievici (1962) durch Differentialthermoanalyse bei 676–678 K beobachtete Umwandlung der β-Form in die α-Form praktisch irreversibel war, und dass Perraud (1974) die Möglichkeit der Umwandlung in umgekehrter Richtung erst nach viermonatigem Erhitzen auf 473 K nachweisen konnte.

Literatur

BJÖRNBERG, A. & HEDMAN, B. (1977). *Acta Chem. Scand. Ser. A*, **31**, 579–584.

BUSING, W. T. & LIBERMAN, D. (1970). *J. Chem. Phys.* **53**, 1891–1898.

CROMER, D. T. & MANN, J. B. (1968). *Acta Cryst.* A**24**, 321–324.

EVANS, H. T. JR (1960). *Z. Kristallogr.* **114**, 257–277.

LUKÁCS, I. & STRUSIEVICI, C. (1962). *Z. Anorg. Allg. Chem.* **315**, 323–326.

MARUMO, F., ISOBE, M., IWAI, S. & KONDO, Y. (1974). *Acta Cryst.* B**30**, 1628–1630.

PERRAUD, J. (1974). *Rev. Chim. Minér.* **11**, 302–326.

Powder Diffraction File (1977). Karte Nr. 27-1402. Swarthmore, Pennsylvania: JCPDS–International Centre for Diffraction Data.

RAMANI, K., SHAIKH, A. M., SWAMINATA REDDY, B. & VISWAMITRA, M. A. (1975). *Ferroelectrics*, **9**, 49–56.

Acta Cryst. (1984). B**40**, 105–109

Crystal Chemistry of Oxide–Chalcogenides. II. Synthesis and Crystal Structure of the First Bismuth Oxide–Sulfide, Bi_2O_2S

BY E. KOYAMA, I. NAKAI AND K. NAGASHIMA

Department of Chemistry, The University of Tsukuba, Ibaraki 305, *Japan*

(*Received* 20 *September* 1983; *accepted* 24 *November* 1983)

Abstract

Bi_2O_2S was synthesized hydrothermally from a stoichiometric mixture of Bi_2O_3 and Bi_2S_3 with 10% NaOH solution as solvent at 673 K and 98 MPa for 3 d. Crystal data: $M_r = 482{\cdot}0$, *Pnnm*, $a = 3{\cdot}874\,(1)$, $b = 11{\cdot}916\,(2)$, $c = 3{\cdot}840\,(1)$ Å, $V = 177{\cdot}28\,(5)$ Å^3, $Z = 2$, $D_x = 9{\cdot}03$ Mg m^{-3}, λ(Mo $K\alpha_1$) $= 0{\cdot}70926$ Å, $\mu = 94{\cdot}6$ mm^{-1}, $F(000) = 396$, $T = 298$ K, $R = 0{\cdot}057$ for 718 independent observed reflections. The Bi atom is coordinated by four O and four S atoms forming a square antiprism. The Bi–O bonds form OBi_4

0108-7681/84/020105-05$01.50

tetrahedra, which share edges to form a BiO layer perpendicular to the *b* axis. The S atoms link the layers into a three-dimensional structure. Close structural relations to Bi_2O_2Se, UOS, and oxide–halides of bismuth are discussed. (The JCPDS Powder Diffraction File No. for Bi_2O_2S is 34-1493.)

Introduction

Oxide–chalcogenides are a group of compounds having a chemical composition intermediate between oxide and chalcogenide. In these compounds, oxygen and chalcogen atoms should be present without forming any anionic group such as sulfate ion.

As an oxide–chalcogenide of a Group V*b* semimetallic element in the periodic table, Sb_2OS_2 is well known as the natural mineral kermesite (Kupčík, 1967). Although the existence of an oxide–sulfide of bismuth is inferred by analogy with Sb_2OS_2, no oxide–sulfide had been known in the Bi–O–S system; and Bi_2O_2Se was the only known oxide–chalcogenide of bismuth (Boller, 1973).

We have carried out a synthetic study of the Bi–O–S system with a view to obtaining a bismuth oxide sulfide. This attempt resulted in the finding of the new oxide–sulfide Bi_2O_2S. The crystal structure analysis has been made to reveal the structural relationships between Bi_2O_2S and other oxide–chalcogenides.

Synthesis

The starting materials used were powders of Bi_2O_3 (purity 99·99%) and Bi_2S_3 (99·99%). They were mixed in a molar ratio of 2 : 1 using an agate mortar. 100 mg of the mixture and 7×10^{-2} cm^3 of 10% NaOH solution were sealed in either a gold or a platinum capsule (length 35 mm, inner diameter 6 mm). The conventional hydrothermal method using Stellite bombs of the test-tube type (length 200 mm, inner diameter 6 mm) was employed. The syntheses were conducted in the temperature range 573 to 773 K at 98 MPa for 1–5 d.

A good single crystal was obtained at 673 K after 3 d. From a synthesis at a temperature above 723 K metallic bismuth was obtained instead of Bi_2O_2S. Bi_2O_2S is blackish silver; it is red by transmitted light. The luster is metallic. The crystal habit is tabular having well developed (010) planes. An electron-microprobe analysis of the crystal gave the chemical formula Bi_2O_2S. The presence of oxygen was confirmed by the direct measurement of the O $K\alpha$ spectrum using the microprobe analyzer. This is the first synthesis of the oxide–sulfide of bismuth.

X-ray powder diffraction data measured by a Gandolfi camera are given in Table 1 together with those for Bi_2O_2Se (Boller, 1973). The similarity of the powder pattern to that of Bi_2O_2Se suggested a structural relationship between the two compounds.

Table 1. *X-ray powder diffraction data for* Bi_2O_2S *and (for comparison) for* Bi_2O_2Se

Bi_2O_2S*					Bi_2O_2Se†		
2θ exp (°)	I/I_o	d_{exp} (Å)	*hkl*	$\Delta2\theta$‡ (°)	d_{exp} (Å)	I/I_o	*hkl*
14·88	40	5·95	020	+0·01	6·11	3	002
24·24	90	3·67	110	+0·08	3·71	18	101
27·47	50	3·25	120	+0·01	3·05	10	004
29·95	70	2·98	040	−0·05	2·82	100	103
32·33	100	2·77	130	+0·05	2·75	32	110
32·81	80	2·73	101	−0·03	2·068	5	105
33·69	40	2·66	111	−0·02	2·040	24	114, 006
45·09	60	2·011	141	+0·02	1·946	15	200
45·62	30	1·989	060	−0·06	1·723	5	211
47·40	50	1·918	002	+0·05	1·637	22	204, 116
50·90	30	1·794	151	+0·02	1·598	43	213, 107
53·81	20	1·704	112	−0·03	1·527	3	008
55·29	50	1·661	221	−0·02	1·417	2	215
57·32	40	1·607	161	−0·07	1·407	6	206
58·46	40	1·579	132	0·00	1·376	4	220
59·22	50	1·560	170	−0·07	1·335	3	118
61·62	10	1·505	250	−0·09	1·290	1	301
62·30	10	1·490	080	−0·04	1·281	3	109
69·25	5	1·357	212	−0·11	1·254	2	224
72·40	40	1·305	261	−0·07	1·232	15	303, 217
80·54	20	1·193	0,10,0	−0·08	1·221	2	0,0,10

* The data were obtained with a 114·6 mm Gandolfi camera, Ni-filtered Cu radiation (λ = 1·5405 Å). The intensities were visually estimated. Corrections were made for the film shrinkage.

† Boller (1973).

‡ $2\theta_{exp}-2\theta_{calc}$.

Experimental

Weissenberg and precession photographs show orthorhombic symmetry with systematic absences $h+l=2n+1$ for $h0l$ reflections, and $k+l=2n+1$ for $0kl$; thus the possible space groups are *Pnn*2 and *Pnnm*; the latter is established by the crystal structure analysis.

The unit-cell dimensions were determined from a least-squares refinement using the setting angles of 22 reflections centered automatically on a Rigaku AFC5 four-circle diffractometer with Mo $K\alpha$ radiation.

The intensity measurement was carried out with a crystal approximately $0{\cdot}15\times0{\cdot}03\times0{\cdot}4$ mm. The intensity data were collected on the Rigaku Rotaflex four-circle diffractometer (operating condition: 50 kV, 160 mA) with graphite-monochromated Mo $K\alpha$ radiation, 2θ–ω scan technique, and a scan speed of 2° min^{-1}. The intensity measurements were repeated up to three times for each reflection unless $\sigma(F_o)/|F_o|$ was less than 0·05. The intensities of three standard reflections were measured every 50 reflections; no significant fluctuation was observed. A total of 906 symmetry-independent reflections were measured within the limit of $2\theta\leq95°$; 718 of which with $|F_o|\geq3\sigma(F_o)$ were regarded as observed and used in the structure determination. The intensity data were corrected for Lorentz, polarization, and absorption effects. The absorption corrections were made by the computer program *ACACA* (Wuensch & Prewitt, 1965). The maximum and minimum absorption factors are 17·86 for 2,13,0 and 1·34 for 200, respectively.

Table 2. *Final atomic coordinates and equivalent isotropic thermal parameters, with e.s.d.'s in parentheses*

$B_{eq} = 4/3(\beta_{11}a^2 + \beta_{22}b^2 + \beta_{33}c^2)$.

	x	y	z	B_{eq} (Å^2)
Bi	0·0806 (1)	0·35677 (4)	0·0	0·97
S	0·0	0·0	0·0	1·26
O	0·5578 (21)	0·2503 (8)	0·0	0·92

The three-dimensional Patterson map indicated the position of the Bi atom. Fourier and difference Fourier syntheses subsequently indicated the positions of the S and O atoms. Least-squares refinement of the atomic positions and isotropic temperature factors using *RFINE*2 (Finger, 1969) yielded $R = 0{\cdot}090$ and $R_w = 0{\cdot}079$ for the observed reflections; $w = 1/\sigma^2(F_o)$. Further refinement using anisotropic temperature factors for all atoms yielded final R and R_w values of 0·057 and 0·044, respectively. The maximum shift in atomic parameters in the last cycle was less than 0·01 times the corresponding standard deviations. A difference synthesis using the final atomic parameters showed no significant residual electron distribution. The final positional and thermal parameters are given in Table 2.* The atomic scattering factors for neutral atoms tabulated by Cromer & Mann (1968) were applied for the calculation. The anomalous-dispersion corrections were taken from *International Tables for X-ray Crystallography* (1974).

Structural description

The crystal structure of Bi_2O_2S is shown in Fig. 1. The O atom is bonded to four Bi atoms, and the OBi_4 tetrahedra share Bi–Bi edges to form an infinite BiO layer perpendicular to the b axis (Fig. 2). The S atoms link the BiO layers into a three-dimensional structure.

The coordination polyhedra and interatomic distances are illustrated in Fig. 3. Selected bond angles are listed in Table 3. The coordination about the Bi atom is a square antiprism comprising four O and four S atoms. In the BiO layer, the average Bi–O bond length is 2·311 Å, which is not significantly different from the Bi–O distances for α-Bi_2O_3 (2·08–2·80 Å) (Malmros, 1970), β-Bi_2O_3 (1·96–2·45 Å) (Aurivillius & Malmros, 1972), and BiO_2Se (2·32 Å) (Boller, 1973). The Bi–O–Bi bond angles for the OBi_4 tetrahedron range from 105·1 to 113·5° with an average of 110·4° (Table 3). These values are close to the ideal tetrahedral angle of 109·78°.

The Bi–S distances for Bi_2O_2S are 3·040 Å (×2) and 3·415 Å (×2). These values belong to the upper limit of the usual Bi–S distances observed in Bi_2S_3 (2·49–3·60 Å) (Kupčík & Nováková, 1970), $PbBi_2S_4$ (2·63–3·12 Å) (Iitaka & Nowacki, 1962), $CuPbBiS_3$ (2·658–3·530 Å) (Ohmasa & Nowacki, 1970), $CuBiS_2$ (2·536–3·692 Å) (Portheine & Nowacki, 1975); therefore the S atom can be considered to form weak bonds with the BiO layers. The Bi–Bi distance between the BiO layers is 3·470 Å. This is less than twice the metallic radius of bismuth, 3·64 Å, suggesting the existence of weak interaction between the Bi atoms.

Table 3. *Selected bond angles (°) with e.s.d.'s in parentheses*

O–Bi–O^{iv}	73·66 (12)	Bi^{iii}–S–Bi^{iii}	68·43 (2)
O^{ii}–Bi–O^{iv}	70·97 (13)	Bi^{iii}–S–Bi^{iv}	73·52 (2)
O–Bi–S^{iii}	82·93 (18)	Bi^{iii}–S–Bi^{v}	64·75 (2)
O^{ii}–Bi–S^{iv}	72·97 (18)	Bi^{iv}–S–Bi^{iv}	78·35 (2)
O^{iv}–Bi–S^{iii}	78·77 (20)	Bi^{iv}–S–Bi^{vi}	64·75 (2)
O^{iv}–Bi–S^{iv}	77·48 (20)		
S^{iii}–Bi–S^{iii}	78·35 (2)	Bi–O–Bi^{i}	113·48 (40)
S^{iii}–Bi–S^{iv}	73·52 (2)	Bi–O–Bi^{iii}	110·15 (23)
S^{iv}–Bi–S^{iv}	68·43 (2)	Bi^{i}–O–Bi^{iii}	105·14 (23)
S^{iii}–Bi–Bi^{vii}	62·86 (2)	Bi^{iii}–O–Bi^{iii}	112·67 (39)
S^{iv}–Bi–Bi^{vii}	52·39 (2)		

Symmetry code: (i) $1+x, y, 0$; (ii) $x-1, y, 0$; (iii) $\frac{1}{2}+x, \frac{1}{2}-y, \pm\frac{1}{2}$; (iv) $x-\frac{1}{2}, \frac{1}{2}-y, \pm\frac{1}{2}$; (v) $\frac{1}{2}-x, y-\frac{1}{2}, \pm\frac{1}{2}$; (vi) $-\frac{1}{2}-x, y-\frac{1}{2}, \pm\frac{1}{2}$; (vii) $-x, 1-y, 0$.

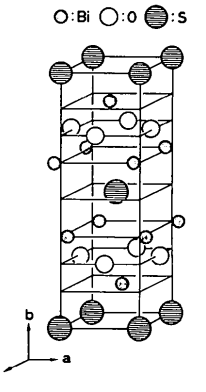

Fig. 1. A view of the crystal structure of Bi_2O_2S.

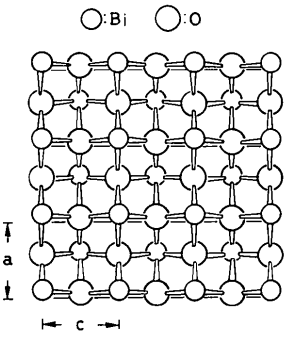

Fig. 2. An infinite BiO layer made up of edge-shared OBi_4 tetrahedra.

* Lists of structure factors and anisotropic thermal parameters have been deposited with the British Library Lending Division as Supplementary Publication No. SUP 39034 (7 pp.). Copies may be obtained through The Executive Secretary, International Union of Crystallography, 5 Abbey Square, Chester CH1 2HU, England.

Table 4. *Reported space groups and cell parameters for oxide–halides of bismuth*

Type	BiOX			$(Bi, M)_2O_2X$			$(Bi, M)_3O_3X_2$	
Compounds	BiOF (*a*)	BiOCl (*b*)	BiOBr (*b*)	$LiBi_3O_4Cl_2$ (*c*)	$NaBi_3O_4Br_2$ (*c*)	$BaBiO_2Cl$ (*d*)	$SrBi_2O_3Br_2$ (*b*)	$CaBi_2O_3Br_2$ (*d*)
Space group	*P4/nmm*	*P4/nmm*	*P4/nmm*	*I4/mmm*	*I4/mmm*	*I4/mmm*	*P4/nmm*	*P4/nmm*
a (Å)	3·747	3·883	3·915	3·840	3·925	4·019	3·982	3·915
c (Å)	6·226	7·347	8·076	12·03	12·55	12·98	20·79	20·75

References: (*a*) Aurivillius (1964); (*b*) Sillén (1941); (*c*) Sillén (1939); (*d*) Sillén & Husberg (1941).

Discussion

Boller (1973) determined the crystal structure of Bi_2O_2Se from the analysis of the powder diffraction data. It is tetragonal, space group $I4mmm$, $a = 3{\cdot}891$, $c = 12{\cdot}21$ Å. Despite the apparent difference in the symmetry of the lattice between Bi_2O_2Se and Bi_2O_2S, a comparison of the two structures has indicated that the structure of Bi_2O_2S is a slightly distorted form of Bi_2O_2Se (Fig. 4). The crystal structure of Bi_2O_2Se is isotypic with the oxide–telluride of lanthanum La_2O_2Te (Ballestracci, 1967) and they belong to the $(Na_{0.25}Bi_{0.75})_2O_2Cl$-type structure (Boller, 1973).

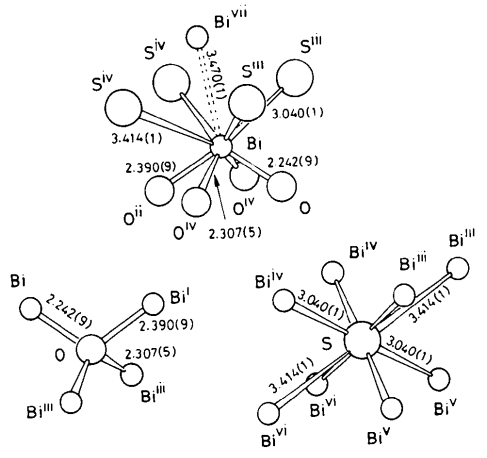

Fig. 3. Coordination polyhedra and interatomic distances (Å) in Bi_2O_2S with e.s.d.'s in parentheses.

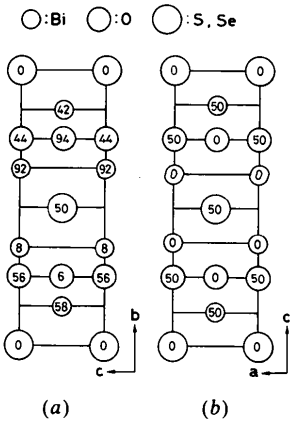

(*a*) (*b*)

Fig. 4. Projection of the structures of (*a*) Bi_2O_2S and (*b*) Bi_2O_2Se along [100]. Numbers give the heights of the atoms in hundredths of the cell dimensions.

The structures composed of the sequences of tetragonal metal–oxygen layers and intervening chalcogen atoms are also found in oxide–sulfides of actinoids, *e.g.* UOS and ThOS (Zachariasen, 1949). The structure of UOS is shown in Fig. 5. The U atom is coordinated by four O and five S atoms. This structure is constructed by infinite UO layers built up of edge-shared OU_4 tetrahedra, and each layer links together through the S atoms. The stacking feature of the UO layers and the S atoms is different from that of Bi_2O_2S; however, both metal–oxygen layers have a similar structure (compare Fig. 1 with Fig. 5). In this way, we find that the structure of Bi_2O_2S is related to those of oxide–chalcogenides of actinoid as well as lanthanoid elements.

As pointed out by Boller (1973), crystal structures composed of the BiO layers and intervening anions are also observed in oxide–halides of bismuth. Table 4 gives the space groups and cell parameters for such compounds. It shows that they belong to the same crystal system (tetragonal), and have similar *a*-axis dimensions. Their structures consist of tetragonal BiO layers similar to that in Bi_2O_2S (Fig. 2). The halogen atoms are located between the layers. The difference among these structures, including Bi_2O_2Se and Bi_2O_2S, is based on the arrangement of the layers and the intervening anions. Here, again, we see a close structural relationship between Bi_2O_2S and the oxide–halides of bismuth.

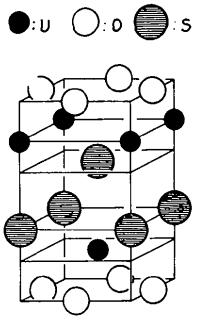

Fig. 5. Crystal structure of UOS.

References

AURIVILLIUS, B. (1964). *Acta Chem. Scand.* **18**, 1823.
AURIVILLIUS, B. & MALMROS, G. (1972). *Trans. R. Inst. Technol. Stockholm*, **291**, 545–562.
BALLESTRACCI, M. R. (1967). *C.R. Acad. Sci.* **264**, 1736–1738.
BOLLER, H. (1973). *Monatsh. Chem.* **104**, 916–919.
CROMER, D. T. & MANN, J. B. (1968). *Acta Cryst.* **25**, 321–323.
FINGER, L. W. (1969). *RFINE2*. Geophysical Laboratory, Carnegie Institution, Washington, DC.
IITAKA, Y. & NOWACKI, W. (1962). *Acta Cryst.* **15**, 691–698.
International Tables for X-ray Crystallography (1974). Vol. IV. Birmingham: Kynoch Press.
KUPČÍK, V. (1967). *Naturwissenschaften*, **54**, 114.
KUPČÍK, V. & NOVÁKOVÁ, L. V. (1970). *Tschermaks Mineral. Petrogr. Mitt.* **14**, 55–59.
MALMROS, G. (1970). *Acta Chem. Scand.* **24**, 384–396.
OHMASA, M. & NOWACKI, W. (1970). *Z. Kristallogr.* **132**, 71–86.
PORTHEINE, J. C. & NOWACKI, W. (1975). *Z. Kristallogr.* **141**, 387–402.
SILLÉN, L. G. (1939). *Z. Anorg. Allg. Chem.* **242**, 41.
SILLÉN, L. G. (1941). *Z. Anorg. Allg. Chem.* **246**, 115.
SILLÉN, L. G. & HUSBERG, G. (1941). *Z. Anorg. Allg. Chem.* **248**, 121.
WUENSCH, B. J. & PREWITT, C. T. (1965). *ACACA*. Absorption correction program.
ZACHARIASEN, W. H. (1949). *Acta Cryst.* **2**, 291–296.

Acta Cryst. (1984). B**40**, 109–114

Electron-Microscopic Study of the Structure of a Metastable Oxide Formed in the Initial Stage of Copper Oxidation. I. Cu_4O

BY R. GUAN,* H. HASHIMOTO AND T. YOSHIDA

Department of Applied Physics, Osaka University, 2-1 *Yamadaoka, Suita, Osaka* 565, *Japan*

(*Received* 6 *July* 1983; *accepted* 30 *November* 1983)

Abstract

In an early stage of oxidation of copper, a metastable copper oxide with the chemical composition Cu_4O has been observed by an atomic-resolution electron microscope. The atomic positions of Cu and O have been studied using electron-microscope images and diffraction patterns interpreted by calculations based on the dynamical theory of electron diffraction. The unit cell of the new oxide Cu_4O belongs to the orthorhombic system with space group *Pmm*2. The lattice parameters are $a = 4{\cdot}02$, $b = 5{\cdot}66$ and $c = 5{\cdot}94$ Å. The volume is approximately two times larger than that of Cu_2O. It is pointed out that at a certain thickness the images of O atoms appear bright and those of Cu atoms do not.

1. Introduction

In the early stages of oxidation of nickel single crystals, Garmon & Lawless (1966) found the existence of an induction period prior to the formation of nickel oxide, which was confirmed by structural changes in the nickel films. They observed a superlattice diffraction pattern similar to that found by Alessandrini & Freedman (1963) for the ordered structures of oxygen in nickel. In the case of copper, Ishii & Hashimoto (1967) observed a superlattice diffraction pattern which seems to be due to a structure intermediate between cuprous oxide and cupric oxide. More recent studies of the oxidation of copper [for a summary see Howie (1981, 1983)] have shown a number of adsorbed-oxygen ordered structures leading after an induction period to the formation of Cu_2O nuclei sometimes with a covering of CuO. Shibahara & Hashimoto (1980) observed a tungsten oxide crystal with a smaller content of oxygen than in WO_2, formed when WO_3 crystals were evaporated in a vacuum of 10^{-4} Pa.

In order to study the non-stoichiometric copper oxide structure observed by Ishii & Hashimoto (1967), the present authors have carried out further observations of the initial stages of copper oxidation and found a new type of copper oxide containing less oxygen than Cu_2O. In this observation, the copper oxide is sometimes found together with its superstructure. The atomic structure has been analysed using a high-resolution transmission electron microscope with interpretation based on the many-beam dynamical theory of electron diffraction. The present paper is concerned with the atomic structure of an oxide having the chemical composition Cu_4O.

2. Specimen preparation and observation

Specimens were prepared in a way similar to that described by Ishii & Hashimoto (1967). A block of pure copper (purity about 99·99%) was rolled into a sheet 70 μm thick. The sheet was annealed at about 923 K in a vacuum of 2·66 Pa for 30 min, and was then electrolytically thinned by a window method in

* Visiting Researcher (1981–1982), on leave of absence from the Institute of Metal Research, Academia Sinica, Shenyang, China.

0108-7681/84/020109-06$01.50